

# Deep-well seismic monitoring based on fiber laser seismometer

Wentao Zhang (张文涛)<sup>1\*</sup>, Wenzhu Huang (黄稳柱)<sup>1,2</sup>, Jian Wu (武健)<sup>1</sup>, and Fang Li (李芳)<sup>1</sup>

<sup>1</sup>Institute of Semiconductors, Chinese Academy of Sciences, Beijing 100083, China

<sup>2</sup>School of Mechanical Engineering, Shijiazhuang Tiedao University, Shijiazhuang 050043, China

\*Corresponding author: zhangwt@semi.ac.cn

Received July 13, 2012; accepted September 4, 2012; posted online December 20, 2012

We present a downhole seismic monitoring system and the field test results using a fiber laser seismometer (FLS). The distributed feedback fiber laser is used as the sensing element of the seismometer. Using the interferometric demodulation system, a minimum detectable acceleration of  $\sim \text{ng}$  is achieved. The FLS is installed in a 400-m-depth well in Puer city, Yunnan Province. A micro-earthquake ( $M=1.2$ ) in Puer area is detected. Compared with the existing underground electrical seismometer, FLS shows a higher signal-to-noise ratio and good reliability, which indicates that the FLS provides a new approach to deep-well seismic monitoring.

OCIS codes: 280.4788, 120.4570.

doi: 10.3788/COL201210.S22802.

Seismometry method provides most of the information for earthquake monitoring and prediction<sup>[1]</sup>. However, with the development of urbanization and industrialization of human society, more and more environmental noise reduces the quality of the traditional seismic observation results. In order to eliminate the ground noise, downhole seismic monitoring becomes an alternative of earthquake monitoring in the future<sup>[2]</sup>. To provide high-precision, stable, and continuous observation in the downhole environment with high temperature and high pressure, the problems such as resistance to high temperature and high pressure, power supply, data collection, and data transmission should be solved<sup>[3]</sup>. Conventional seismograph includes pendulum seismograph, moving-coil seismograph, and piezoelectric seismograph. These electric sensors are easy to be interfered by electromagnetic interference (EMI) and be damaged by the lightning strike.

Fiber optic sensors have been developed for more than thirty years and have many applications in many fields due to their high sensitivity, wide dynamic range, immunity to EMI, and feasibility in multiplexing<sup>[4]</sup>. It has been demonstrated that earthquake monitoring can be performed by using fiber optical accelerometers which detect the earthquake induced acceleration<sup>[5]</sup>. However, for borehole seismic monitoring, an ultra thin dimension is preferred because the diameter of the borehole is limited within several centimeters. Fiber laser sensors, since it is first reported in 1990's, offers an alternative approach to micro-seismic wave detection with ultra-thin dimension<sup>[6-8]</sup>. These fiber laser sensors make it possible to build a 'seismometer array' with diameters of only several centimeters in a borehole down to several thousand meters.

In this letter, we report the field demonstration of a fiber laser seismometer (FLS) based on fiber laser accelerometers (FLAs). The FLA design, the interrogation system, and the field test results are presented.

Recently, optical fiber sensor based on distributed feedback (DFB) fiber laser has attracted considerable research interests. The DFB fiber laser consists of a length

of  $\text{Er}^{3+}$ -doped or  $\text{Yb}^{3+}/\text{Er}^{3+}$ -co-doped fiber written in Bragg gratings. By introducing a  $\pi$  phase shift, the grating resonance is moved to the center of the grating reflection band, which makes DFB fiber laser operate robustly in a single longitudinal mode. The lasing wavelength of DFB fiber laser is determined by the central wavelength in the reflective spectrum of phase-shifted grating, shown as

$$\lambda_B = 2n_{\text{eff}}\Lambda, \quad (1)$$

where  $\lambda_B$  is the lasing wavelength,  $\Lambda$  is the period of grating, and  $n_{\text{eff}}$  is the effective index of fiber core. The period  $\Lambda$  and the effective reflective index  $n_{\text{eff}}$  are changed with the environmental conditions, such as strain, temperature, and seismic wave.

The laser full-width at half-maximum (FWHM) line-width was measured by using self-heterodyne method with a 25-km-long delay fiber and a fiber coupled acousto-optic modulator (55 MHz). For the usual case of Lorentzian-shaped spectrum, the measured FWHM line-width was about 3 kHz (Fig. 1). The ultra-narrow line width of DFB fiber laser will result in a low equivalent noise level when using interferometric demodulation method.

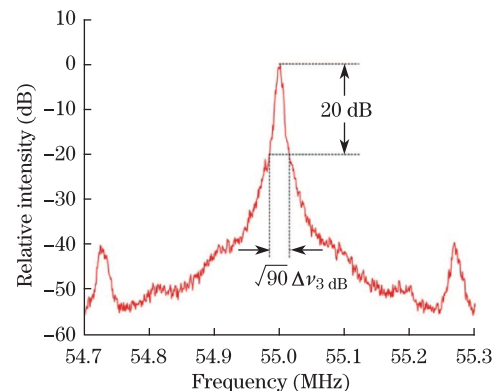


Fig. 1. Line width test result of DFB fiber laser.

Figure 2 shows the principle of the multiplexing of DFB fiber laser sensor array. The fiber lasers are pumped with a 980- or 1480-nm semiconductor laser. The output laser with different wavelengths is de-multiplexed by a dense wavelength division multiplexing (DWDM) in the demodulation system.

The proposed ultra thin-FLA<sup>[9,10]</sup> has been improved to become a seismometer. As shown in Fig. 3(a), two diaphragms (diaphragm A and B), installed on the sensor shell, are working as the elastic element. The mass, which is installed between the diaphragms, has been enlarged to make the nature frequency lower to detect the low frequency earthquake signal. The fiber laser is anchored at the upper cover and diaphragm B. The FLA is encapsulated in a stainless steel shell with fiber optic temperature sensors. When the seismic wave induces vibration of the stainless steel shell, the DFB fiber laser will have a center wavelength shift due to the axial strain induced by the inertial force of the mass.

Figure 3 shows the schematic and the photo of FLA we have improved. The outer diameter of the FLA is 12 mm. The length of the FLA is about 85 mm. So the acceleration sensitivity of the FLA can be written as<sup>[10]</sup>

$$M_a = \frac{\Delta\lambda_B}{a} = \frac{0.78\lambda_B m \left[ 1 - \left(\frac{r}{R}\right)^2 \frac{1 - \left(\frac{r}{R}\right)^2 + 4\ln^2\left(\frac{r}{R}\right)}{1 - \left(\frac{r}{R}\right)^2} \right]}{\frac{32\pi DL}{R^2} + E_f A \left[ 1 - \left(\frac{r}{R}\right)^2 \frac{1 - \left(\frac{r}{R}\right)^2 + 4\ln^2\left(\frac{r}{R}\right)}{1 - \left(\frac{r}{R}\right)^2} \right]}, \quad (2)$$

in which  $D = \frac{E_m t^3}{12(1-\nu^2)}$ , where  $m$  is the mass,  $a$  is the acceleration,  $A$  is the cross area of the fiber,  $E_f$  is the Young's modulus of the fiber,  $t$  is the thickness of the diaphragm,  $R$  is the radius of the diaphragm,  $r$  is the contact radius of the mass and the diaphragm,  $E_m$  is the Young's modulus of the diaphragm,  $\nu$  is the Poisson's ratio of the diaphragm,  $L$  is the length of the fixed fiber, and  $P_e=0.22$  is the effective photo-elastic constant of the fiber.

Equation (2) provides a guidance direction for the design and improvement of FLS. It can be found that ratio of the radius of the diaphragm and the contact radius of the mass and the diaphragm have significant influence on the sensitivity of the FLA as well as the thickness of the diaphragm. The material properties and geometric parameters of FLA are shown in Table 1. The sensitivity of FLA is calculated to be about 64 pm/g.

The interrogation of FLS is achieved by using (phase generated carrier, PGC) demodulation<sup>[11]</sup>, which is shown in Fig. 4. The unbalanced interferometer can convert the FLS's wavelength shift to the interferometer phase shift, and the wavelength demodulation can be achieved with high resolution PGC algorithm.

To local the earthquake source and get more information of the earthquake, seismic waves both at high

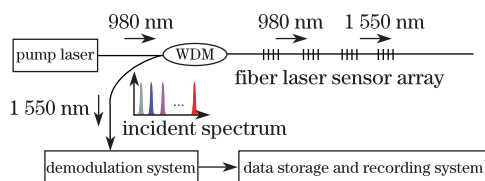


Fig. 2. Work principle diagram of DFB fiber laser sensor array measuring system.

Table 1. Material Properties and Geometric Parameter of FLA

Parameters	Value
$A$ (mm <sup>2</sup> )	0.0123
$E_f$ (GPa)	72
$t$ (mm)	0.05
$R$ (mm)	4.5
$r$ (mm)	1.5
$m$ (g)	10.6
$E_m$ (GPa)	112
$\nu$	0.37
$L$ (mm)	45
$\lambda_B$ (mm)	1500

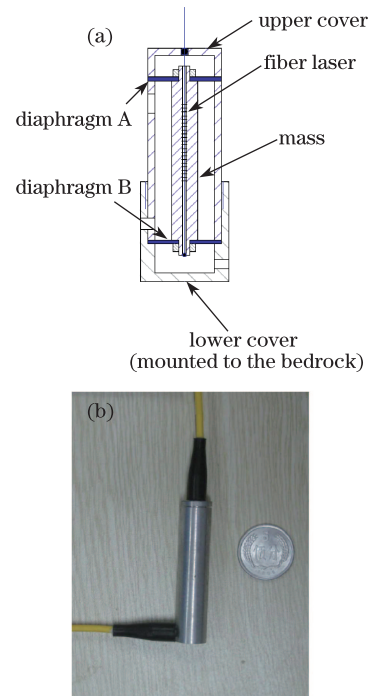


Fig. 3. (a) Schematic and (b) photo of FLA.

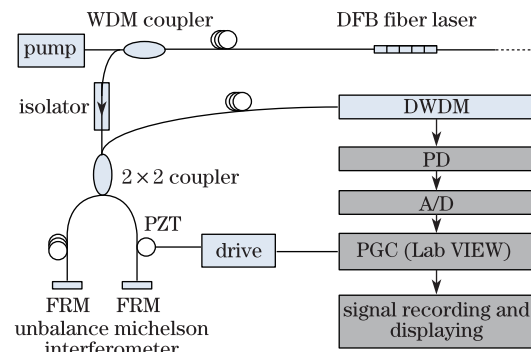


Fig. 4. Schematic of the wavelength demodulation for FLS.

frequency and low frequency are necessary. So the FLS should have a flat frequency response as well as a high sensitivity. The sensitivity of the FLA inside the FLS is tested in the laboratory before the field demonstration.

The calibration of FLS is carried out according to GB/T 13823 (the calibration method of vibration and impact sensor). The test result (Fig. 5) shows a sensitivity of 50 pm/g and a flat frequency response within 10–300 Hz. The difference between the calculated result and the test result is supposed to be the error in the manufacture of the sensor.

Figure 6 is the test results of the bottom noise of the high resolution wavelength demodulation system in the 5–2000-Hz band range. It can be found that the equivalent noise level is  $1 \times 10^{-6}$  pm/(Hz)<sup>1/2</sup>. With a sensitivity of 50 pm/g, a minimum detectable signal of 20 ng is achieved.

The deep-well earthquake monitoring system using FLS is shown in Fig. 7. The fiber laser sensor demodulation system can be put in the monitoring room in the monitoring station. The FLS is cemented at the bottom of the deep well, which is connected to the demodulation system by the optical cable.

Ideally, the FLA is not insensitive to transverse strain.

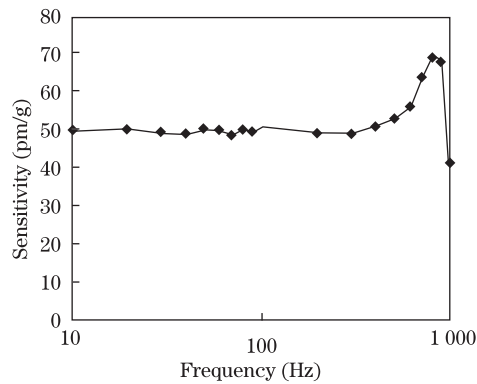


Fig. 5. Sensitivity test result of FLS.

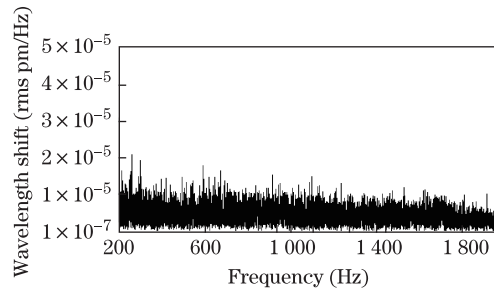


Fig. 6. Noise floor of the high-accuracy demodulator.

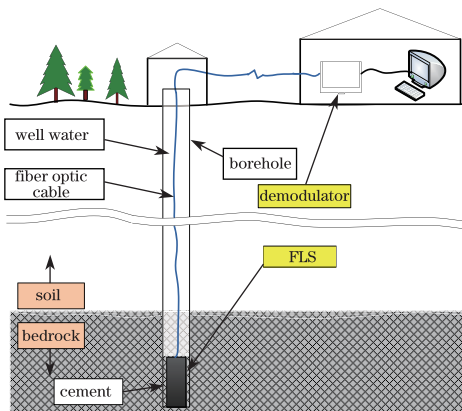


Fig. 7. System of earthquake monitoring based on FLS.

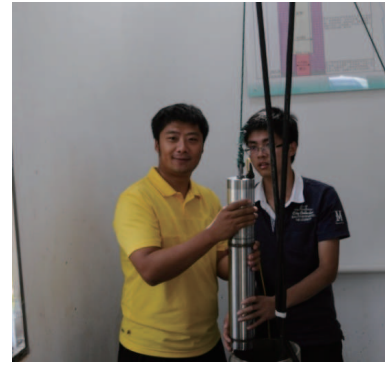


Fig. 8. Photo of the experiment using FLS in Puer area.

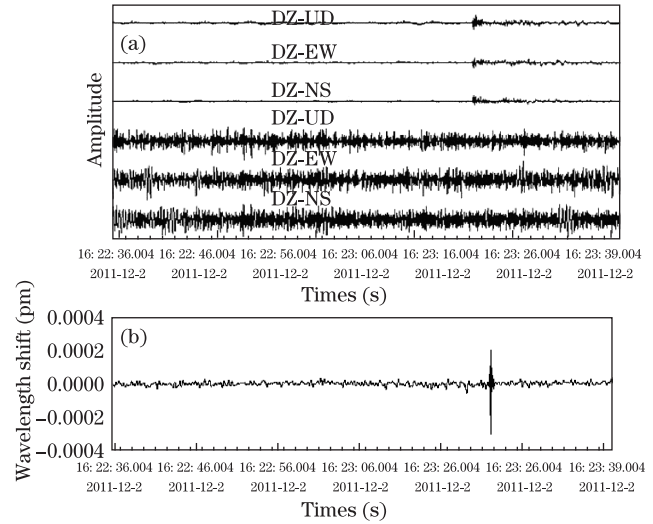


Fig. 9. Earthquake record (16:23, 2011-12-02) by (a) moving-coil seismometer and (b) FLS.

So a three-axis FLA is necessary for earthquake locating. The proper installation of FLS is also important for determine the direction of seismic wave. The field test is carried out in Puer area in Yunnan Province. The FLS is put into a borehole with a depth of 400 m, together with a moving-coil seismometer. Both of the FLS and the moving-coil seismometer are cemented in the well. The photo of the FLS and the borehole is shown in Fig. 8.

Figure 9 is the test result of the FLS in Puer area, Yunnan Province. An earthquake happened at 16:23 Dec 2nd 2011 was recorded by the FLS (in the vertical direction) and the moving-coil seismometer. It can be found from Fig. 8 that the FLS have a better SNR than the moving-coil seismometer. This may have two reasons. Firstly, the FLS system has the immunity to EMI. So the quality of the data is better. Secondly, the FLS system has a lower equivalent noise level.

In conclusion, we present a downhole seismic monitoring scheme using FLS to meet the needs of deep-well seismic monitoring. We show the field demonstration of earthquake monitoring using a fiber laser borehole seismometer. It can be found from the results that the FLS system has a lower equivalent noise level, a higher SNR, and good reliability, which indicates that the FLS can provide another approach to the deep-well seismic monitoring.

This work was supported by the National Natural Science Foundation of China (Nos. 41074128 and 40974022) and the Beijing Science & Technology New Star Program (No. 2010B055). The authors wish to thank Mr. Baorong Bai for the help in the experiment.

## References

1. X. Chi, Progress in Geophys. (in Chinese) **22**, 1164 (2007).
2. G. Liu, S. Dong, and X. Chen, Acta Geologica Sinica **84**, 909 (2010).
3. H. Li and H. Li, Acta Geologica Sinica **84**, 895 (2010).
4. P. Nash, Radar Sonar Navig. **43**, 204 (1996).
5. D. L. Gardner, T. Hofler, S. R. Baker, R. K. Yarber, and S. L. Garrett, J. Lightwave Technol. **5**, 953 (1987).
6. D. J. Hill, P. J. Nash, S. D. Hawker, and I. Bennion, Proc. SPIE **3483**, 301 (1998).
7. S. Foster, A. Tikhomirov, M. Milnes, J. van Velzen, and G. Hardy, in *Proceedings of International Conference on Optical Fibre Sensors* 627 (2005).
8. F. Li, J. He, T. W. Xu, W. T. Zhang, Y. J. Wang, and Y. L. Liu, Infrared Laser Engineering (in Chinese) **38**, 1025 (2009).
9. W. Zhang, Y. Liu, F. Li, and H. Xiao, Journal Lightwave Technol. **26**, 1349 (2008).
10. W. Zhang, X. Li, F. Zhang, F. Li, and Y. Liu, Proc. SPIE **7634**, 76340L (2009).
11. H. Xiao, F. Li, and Y. Liu, Laser Optoelectronics Progress (in Chinese) **44**, 50 (2007).